Using high-density UAV-Lidar for deriving tree height of *Araucaria Angustifolia* in an Urban Atlantic Rain Forest

Ernandes Macedo da Cunha Neto[a]*; Franciel Eduardo Rex[a]; Hudson Franklin Pessoa Veras[a]; Marks Melo Moura[a]; Carlos Roberto Sanquetta[a]; Pâmela Suélen Käfer[b]; Mateus N. I. Sanquetta[a]; Angelica Maria Almeyda Zambrano[c]; Eben North Broadbent[d]; Ana Paula Dalla Corte[a]

[a]Department of Forest Engineering, Federal University of Paraná (UFPR), Curitiba, PR, Brazil, e-mails/ORCIDs:

netomacedo878@gmail.com. https://orcid.org/0000-0001-6775-0365.

francielrexx@gmail.com. https://orcid.org/0000-0003-0876-8500.

hudsonveras@gmail.com. https://orcid.org/0000-0002-0203-1914.

marksmoura@yahoo.com.br. https://orcid.org/0000-0002-2964-8527.

carlossanquetta@gmail.com. https://orcid.org/0000-0001-6277-6371.

mateus.sanquetta@gmail.com. https://orcid.org/0000-0002-2633-5509.

anapaulacorte@gmail.com. https://orcid.org/0000-0001-8529-5554.

[b]State Research Center for Remote Sensing and Meteorology, Federal University of Rio Grande do Sul (UFRGS), Porto Alegre, RS, Brazil, e-mail: pamelaskafer@gmail.com, https://orcid.org/0000-0002-4932-8715.

[c]Spatial Ecology and Conservation Lab, Latin American Studies, University of Florida, Gainesville, FL, USA, e-mails: aalmeyda@ufl.edu, https://orcid.org/0000-0001-5081-9936.

[d]Spatial Ecology and Conservation Lab, School of Forest Resources and Conservation, University of Florida, Gainesville, FL, USA, e-mails: eben@ufl.edu, https://orcid.org/0000-0002-4488-4237.

*Corresponding author: Tel: +55(91) 98283-6532; E-mail: netomacedo878@gmail.com

Using high-density UAV-Lidar for deriving tree height of *Araucaria Angustifolia* in an Urban Atlantic Rain Forest

Abstract: Urban forest remnants contribute to climate change mitigation by reducing the amount of carbon dioxide in urban areas. Hence, understanding the dynamics and the potential of urban forests as carbon pools is crucial to propose effective policies addressing the ecosystem services' maintenance. Remote sensing technologies such as Light detection and ranging (Lidar) are alternatives to acquire information on urban forests accurately. In this paper, we evaluate a UAV-Lidar system's potential to derive individual tree heights of *Araucaria angustifolia* trees in an Urban Atlantic Forest. Additionally, the influence of point density when deriving tree heights was assessed (2,500, 1,000, 500, 250, 100, 50, 25, 10 and 5 returns.m^{-2}). The UAV-Lidar data was collected with the GatorEye Unmanned Flying Laboratory 'Generation 2'. The UAV-Lidar-derived and field-based tree heights were compared by statistical analysis. Higher densities of points allowed a better description of tree profiles. Lower densities presented gaps in the Crown Height Model (CHM). The highest agreement between UAV-Lidar-derived and field-based tree heights (r = 0.73) was noticed when using 100 returns.m^{-2}. The lowest *rRMSE* was observed for 50 returns.m^{-2} (8.35%). There are no explicit differences in derived tree heights using 25 to 2,500 returns.m^{-2}. UAV-Lidar data presented satisfactory performance when deriving individual tree heights of *Araucaria angustifolia* trees.

Keywords: Forest inventory, GatorEye, Remote Sensing, Urban landscape.

1. Introduction

Exposure to nature has been linked to human health as they promote mental and physical health (Jim, 2004). The increasing demand for resources needed to manage people's lives and support modern life pressures resulted in several diseases such as stress, cardiovascular disease, stroke, depression, and asthma (Jiang et al., 2014; Tooke et al., 2009). Thus, urban green areas have been reported as effective in promoting mental and physical health.

Urban green areas such as gardens, parks, and forest remnants play an essential role by providing several ecosystem services. These areas mitigate the heat island phenomena, regulate microclimate, protect biodiversity, improve life quality, and reduce the impacts of air pollution (Alonzo et al., 2014; La Rosa and Wiesmann, 2013; Tigges et al., 2013; Zhang et al., 2015). Besides, urban forest remnants contribute to climate change mitigation by stocking carbon dioxide in their biomass (Liu and Li, 2012; McHale et al., 2007). Hence, understanding the dynamics and the potential of urban forests as carbon pools is crucial to propose effective policies addressing the ecosystem services' maintenance (Alonzo et al., 2016; Doukalianou et al., 2020; Zhang et al., 2020;).

Unfortunately, there is a lack of studies assessing urban forests, resulting in a poor understanding of these areas and their environmental contribution. Usually, these assessments are based on a limited set of plots randomly distributed within the remnants (Nowak et al., 2008). In some cases, aerial images have been used to support sampling designs, given the difficulty in conducting full-cover inventories (Zhang et al., 2010). Moreover, the massive range of vegetation types and single-species dominance hinder these assessments, requiring, thus, exhaustive field and financial costs to comprehensive data collection (Means et al., 2000).

Given this scenario, remote sensing technologies emerge as an alternative to provide spatially extensive data, combining high temporal resolution and low cost. These technologies have been used in forests with complex structures, such as urban forest remnants (Alonzo et al., 2016; Donoghue and Watt, 2006; Hall et al., 2006). Combining field-based and remote sensing data seems to be the best practice (Cunha Neto et al., 2020, 2019), especially when high-resolution data is available. Recent studies indicated Light Detection and Ranging (Lidar) active sensors as promising tools to obtain tree parameters (Corona et al., 2012; Næsset and Økland, 2002; Oliveira et al., 2020) and design vegetation structure 3D maps (Guo et al., 2017; Safaie et al., 2021). Additionally, unmanned aerial vehicles (UAVs) have revolutionized earth and environmental research by their broad and fast application at low costs (Anderson and Gaston, 2013; Hao et al., 2020; Vivoni et al., 2014; Zhou and Zhang, 2020). In forest assessments, ccs provide flexibility regarding spatial and temporal scales (Feng et al., 2015).

Recent studies matched Lidar data and UAV technologies, resulting in an exciting combination of very high-resolution data from local to regional scales at a significantly lower survey cost (Asner et al., 2013; Hao et al.,2021; Li, Li and Feng, 2021; Peng et al., 2021; Wallace et al., 2012). Some researchers addressed their efforts in order to suggest modeling approaches for urban forests using Lidar data or integrating Lidar with optical images (Haala and Brenner, 1999; Holopainen et al., 2013; Liu et al., 2013; Saarinen et al., 2014; Whang et al., 2021; Wu et al., 2013). However, the application of UAV-Lidar to obtain individual tree data in urban forests still lacks research.

The UAV-Lidar system seems to be more convenient over the Airborne Lidar (Airborne Laser Scanner - ALS), as it presents lower cost, more accessible transportation, and a higher density of points (> 800 returns per m^{-2}). Thus, UAV-Lidar can provide digital models with higher resolution (Guo et al., 2017; Sankey et al., 2012, 2010). However, the understanding of point density influence when predicting individual tree parameters is still limited (Ruiz et al., 2014; Sankey et al., 2017). Hence, there is an evident need for investigating this influence by deriving individual tree metrics using the UAV-Lidar system (Guo et al., 2017; Jakubowski et al., 2013), mainly because these metrics are employed in allometric equations (Sanquetta et al., 2018). Thus, this paper investigates the potential of using UAV-Lidar data to derive the total tree height of *Araucaria angustifolia* (Bertol.) Kuntze (Brazillian pine) individuals in an urban remnant of the Atlantic Rain Forest. We also intended to evaluate the influence of point density on estimates' accuracy.

2. Material and Methods

2.1 Study area description

The study area is an urban forest remnant located in Curitiba, State of Parana, southern Brazil. UAV-Lidar data collection was performed to cover approximately 150,000 m² (15 ha) of a very distinguished forest formation (so-called Araucaria Forest) from the Brazilian Atlantic Rain Forest (Maas et al. 2020). The study area is located within the coordinates 25º26’50” and 25º27’33” S and 49º14’16” and 49º14’33” W (Fig. 1). The elevation ranges from 893.34 to 925.46 m (Machado et al., 2012). The region’s climate zone is classified as subtropical humid mesothermal (Cfa), with an undefined dry season, and an average temperature in the hottest month of 22°C, while the temperature is close to 12°C in the coldest month (Peel et al., 2007).

The Araucaria Forest is a specific forest formation resulting from the interaction between Austral-Andean and tropical Afro-Brazilian floras (Maas et al. 2020). It is one of the most diverse forests across the globe and is considered one of the "hottest" hotspots of biodiversity (Laurance, 2009; Myers et al., 2000). Although the Araucaria forest has been severely devastated in the past few decades, the Brazilian pine stands out as a single emerging tree species (Carlucci et al., 2021; Lira et al., 2021; Pozzan et al., 2020).

Fig. 1 is here

2.2 Forest inventory

The field-based data were collected in a field cruise performed in November 2019. A total of 171 Brazilian pine trees were measured regarding their circumference at 1.30 m height above the ground using a millimetric tape and later transformed into *dbh* (diameter at 1.30 m height above the ground). The tree height (*h*) was always measured with a Haglöf Vertex IV, while the geographical position was recorded using a Garmin GPS, model 62CSX.

2.3 Lidar data collection

The UAV-Lidar data was collected using the GatorEye Unmanned Flying Laboratory 'Generation 2' (data available for download at www.gatoreye.org). The GatorEye 'Generation 2' comprises a modified Phoenix Scout Ultra system with a STIM300 Internal Motion Unit (IMU), an L1/L2 dual-frequency GNSS receiver, an SSD drive, and a Velodyne 32c Ultra Puck. The Velodyne 32c accommodates 32 lasers with a range up to 220 m, providing an along-track field of view (FOV) of 40 degrees and 360 degrees of cross-track data. The post-processing kinematic (PPK) flight trajectory was produced with on-site base station data in Novatel Inertial Explorer software, providing an point cloud absolute spatial accuracy of approximately 5 cm RMSE (Wilkinson et al., 2019). The flight height was 75 m (aboveground level) at a speed of 10 $m.s^{-1}$ and an approximate horizontal distance between the adjacent flight lines of 40 m, producing a high-density Lidar point cloud totaling 172,800 points and 2,781,56 $returns.m^{-2}$.

2.4 Lidar data processing

The UAV-Lidar data was processed using the rLiDAR (Silva et al., 2017a) and lidR (Roussel and Auty, 2019) packages in software R version 3.6.1 (R Core Team, 2019). In order to evaluate the influence of point density when refining tree height, we thinned the original point cloud and defined nine scenarios as follows: 2,500, 1,000, 500, 250, 100, 50, 25, 10, and 5 returns.m-². The '*lasfilterdecimate*' function was used for this purpose. Then, we designed eight new normalized clouds according to ground points to generate both Digital Terrain Model (DTM) and Crown Height Model (CHM). The functions '*lasground*', '*lasnormalize*', '*grid_terrain*', and '*grid_canopy*' were used.

The '*lasground*' function classified the point cloud into ground and non-ground, by that we use the CSF algorithm (Zhang et al., 2016), while '*lasnormalize*' generated normalized LiDAR point clouds. The functions '*grid_terrain*', and '*grid_canopy*' obtained the Digital Terrain Model (DTM) and Crown Height Model (CHM), both with a resolution of 0.5 m. In '*grid_terrain*' we use 'tin' algorithm and '*grid_canopy*' we use points-to-raster method.

The function '*CHMsmoothing*' was used as a smoothing filter (gaussian with sigma 0.7) to remove possible noises and trees with a height below those measured in the field. Smoothed CHMs were combined with normalized clouds to derive the treetop and assess individual tree heights with the '*tree_detection*' function by local maximum filter (lmf) algorithm (Popescu and Wynne, 2004). This algorithm was used because there is a biological consistency between the highest point in the point cloud and the treetops. Additionally, in the data curation, tree height was also estimated based on treetops, using the Vertex IV. Each treetop and geographical position allowed the identification of each Brazilian pine tree. A spatial join was applied to join by position the heights measured in the field and derived by UAV-Lidar.

2.5 Assessment of derived heights

The accuracy of each point density was evaluated by comparing UAV-Lidar derived tree height and field-based data. The Pearson correlation coefficient (r), as well as the root mean squared error (*RMSE*) and bias were assessed (Eq. 1 to 3) (Sanquetta et al. 2018). Additionally, graphical analysis was conducted to examine the residual pattern and agreement between UAV-Lidar and field-based values. The chi-squared test was employed to identify explicit differences (95% probability) – (Eq. 4). Duncan test was used to determine the best-performed point density (95% probability).

$$r = \frac{\sum_{i=1}^{n}(yi - \bar{y})(\hat{yi} - \bar{\hat{y}})}{\sqrt{\sum_{i=1}^{n}(yi - \bar{y})^2 \sum_{i=1}^{n}(\hat{yi} - \bar{\hat{y}})^2}} \tag{1}$$

$$rRMSE\ (\%) = \frac{100}{\bar{y}} \sqrt{\frac{\sum_{i=1}^{n}(y_i - \hat{y}_i)^2}{n}} \tag{2}$$

$$Bias\ (\%) = \frac{100}{\bar{y}} \frac{\sum_{i=1}^{n}(y_i - \hat{y}_i)}{n} \tag{3}$$

$$\chi^2 = \frac{\Sigma_{i=1}^{n}(\hat{y}_i - yi)^2}{yi} \tag{4}$$

Where: y_i is the field-based tree height of the i*th* tree; $\bar{y}$ is mean of field-based tree heights; $\hat{y}_i$ is UAV-Lidar derived tree height of the i*th* tree; $\bar{\hat{y}}$ is the mean of UAV-Lidar derived tree heights; and *n* is the sample size (171 trees).

3. Results

3.1 Derived tree heights

UAV-Lidar derived tree heights were assessed by descriptive analysis. Mean, minimum, and maximum, as well as the standard deviation, are shown in Table 1. A slight trend to higher mean values was noticed as the pulse density increased. The maximum tree height, however, decreased with higher densities.

Table 1 is here

The tree height distribution pattern was maintained when using densities from 100 to 2,500 returns.m^{-2}. Lower densities (5 and 10 returns.m^{-2}) presented different patterns, in which lower values were observed, and the curves differed from field-based data (Fig. 2).

Fig. 2 is here

3.2 Tree profile assessment

Most Lidar returns came from tree crowns, which is mainly caused by the nature of Brazilian pine's architecture. As expected, higher pulse densities provided better descriptions of tree profile. Lower densities poorly captured the stem profile (Fig. 3). This fact may probably affect tree height derivation since smaller variations were observed for derived heights in lower densities (> 50 returns.m^{-2}), as shown in Table 1.

Fig. 3 is here

3.3 Digital Terrain and Crown Height Models

Although pulse density proved to be critical in describing the tree profile, digital terrain models were less affected as the pulse density decreased (Fig. 4). All DTM produced for pulse densities higher than 50 returns.m^{-2} (Figs. 4b-f) showed a similar pattern compared to 2,500 returns.m^{-2} (Fig. 4a), except for 100 returns.m^{-2} (Fig. 4e). Hence, we noticed higher differences for lower densities (> 50 returns.m^{-2}), in which these differences ranged from -2.5 and 2.5 m (Figs. 4g-i).

Fig. 4 is here

Fig. 5a displays the CHM regarding 2,500 pulse density. We noticed small differences among CHM generated for higher densities (1,000, and 500 returns.m^{-2}) – Figs. 5b and 5c. Intermediate densities (*i.e.*, 250 and 100 returns.m^{-2}) presented slightly higher differences (Figs. 5b-c), ranging from -7.5 to 2.5 m. It is worth noting that smaller densities showed a higher amplitude of differences, with extreme values of -15 m (Figs. 5f-i).

Fig. 5 is here

3.4 Performance of UAV-Lidar derived tree heights

Although higher densities provided better descriptions of tree profiles, all statistics were enhanced as pulse density decreased, reaching the best statistics when using 50 (r = 0.73, *rRMSE* = 8.35%, and Bias = -4.09%) to 100 (r = 0.72, *rRMSE* = 8.51%, and Bias = -4.74%) returns.m^{-2} (Table 2). Lower densities (5 to 25 returns), however, presented the poorest results. Meanwhile, no explicit differences were observed when compared to field data, according to the Chis-square test.

Table 2 is here

A slight trend of overestimation was noticed in all cases (Fig. 6). We noticed that derived tree heights were generally overestimated. Smaller tree heights were better predicted as the densities increased. The slope between derived and field was illustrated and presented similar patterns among pulse densities (Fig. 6).

Fig. 6 is here

The Duncan test indicated that UAV-Lidar derived tree heights using 2,500 returns.m^{-2} differed from the densities of 10 and 5 returns.m^{-2}. There is no explicit difference when deriving the total tree height of Brazilian pine when using 25 - 2,500 returns.m^{-2} (Fig. 7).

Fig. 7 is here

4. Discussion

This study indicated the potential of UAV-Lidar in deriving the individual tree height of Brazilian pine trees in an Urban Atlantic Forest. UAV-Lidar-derived tree heights presented a strong relationship with field-based data (r ranging from 0.44 to 0.73), as shown in Table 2. The evaluation of different point densities suggested that low densities could provide similar distribution compared to field-based values (10 and 25 returns.m^{-2}). The particular tree architecture of Brazilian pine trees may have influenced the results, as they do not have a well-defined treetop but rather a cup shape. Field-based tree height is also influenced by tree architecture, especially when using hypsometers. We believe that a higher density of points could provide more accurate tree heights, which may be impractical to perform in traditional field methods since the operator's experience and environmental and stand conditions can lead to gross errors.

A high density of points is also necessary for reproducing accurate 3D maps (Guo et al., 2017), as it captures detailed data from forest structure. Hence, it is possible to design a detailed description of forest surface and structure and high-resolution 3D maps (Campbell et al., 2018; Hamraz et al., 2017; Kükenbrink et al., 2017). Hamraz et al. (2017) suggested that densities higher than 100 returns.m^{-2} are necessary to describe the tree profile in natural forests.

Accurate UAV-Lidar-derived tree heights are closely related to DTM accuracy (Watt et al., 2014, 2013). A few studies suggested that designing DTMs with low densities (> 5 returns.m^{-2}) resulted in satisfactory accuracy when deriving forest metrics (Rex et al., 2019; Silva et al., 2017b; Wannasiri et al., 2013). However, for designing CHMs, lower densities proved to be inefficient (Fig. 5), as suggested by Li et al. (2013).

In our study, no explicit increase in accuracy was observed when point density increased, corroborating with Ruiz et al. (2014). These authors pointed out that accuracy and density are not directly proportional. Differently, Silva et al. (2017c) and Li et al. (2013) noticed greater accuracy and precision with higher densities. Jakubowski et al. (2013) used a Lidar point cloud with 57 returns.m^{-2} and reported that, at the plot level, high precision does not require a high density of returns. However, it is necessary for individual tree assessments. Point densities greater than 25 returns.m^{-2} behave well when deriving tree heights if Brazilian pine (*rRMSE* lower than 9%), despite a slight tendency of overestimation. Therefore, different point densities should be evaluated in each particular condition

Wannasiri et al. (2013) used an airborne Lidar in Mangroves in Thailand and found a bias of -5.7% and *rRMSE* of 19.4% with 2.7 returns.m^{-2} when deriving tree heights. Guo et al. (2017) used a UAV-Lidar (293.4 returns.m^{-2}) in Mangroves, China. These authors observed an *RMSE* of 1.08 m in a population of 2.8 m (mean stand height), equivalent to an *rRMSE* of 38.57%. Yin and Wang (2019) using a UAV-Lidar (average density of 91 returns.m^{-2}) found a bias between -3.5% and -9.4% and *rRMSE* between 6.3% and 14.3%. These studies reinforce the satisfactory results found in this study and the potential of the GatorEye Unmanned Flying Laboratory ‘Generation 2’.

Although the future of UAV-Lidar technology as a source of 3D forest information seems to be very promising, it should be emphasized that it is still necessary to define the minimum point density to obtain forest metrics with higher precision and accuracy since it is possible to reduce the speed and/or height of the flight, in order to optimize the data collection (Ruiz et al., 2014). High-density point clouds imply higher financial costs and machine effort for effective processing, requiring computers with high processing and storage capacity (Aji et al., 2013; Hongchao and Wang, 2011; Werder and Krüger, 2009).

Finally, deriving individual tree metrics from UAV-Lidar data proved to be a promising approach, especially in green urban areas, such as the protected remnants of Araucaria Forest in Brazil. Traditional methods, mostly based on destructive methods, are impracticable. Thus, the use of UAV-Lidar seems a promising tool to assist volume, biomass, and carbon prediction. Future studies are needed to provide an additional evaluation contrasting UAV-Lidar derived tree height with direct measurements and deriving other individual tree metrics.

Conclusion

This study investigated the potential of using UAV-Lidar data to derive *A. angustifolia* trees' height in an Urban Atlantic Forest. Complementary, the effect of the density of the points in obtaining its total height was assessed.

High accuracy was noticed when deriving individual tree heights, regardless of the density of points. We found that the point cloud can be reduced up to 25 returns.m^{-2}, with no accuracy loss. However, it is suggested that different point densities be evaluated regarding specific conditions of forest typology and structure, and study purposes.

The structure of the tree's crown directly influenced the height estimate obtained by UAV-Lidar, however, smaller point densities can be used without influencing the accuracy of its height. DTMs with low point densities prove to be efficient for estimating forest metrics, however these densities are not very effective for projecting CHMs

6. Acknowledgements

The authors are very grateful to the Conselho Nacional de Desenvolvimento Científico e Tecnológico (CNPq, Brazil) for providing a scholarship to the first author. The authors also thank the Spatial Ecology and Conservation (SPEC) Lab at the University of Florida who funded and collected the GatorEye Unmanned Flying Laboratory Lidar data, with support from the USDA National Institute of Food and Agriculture McIntire-Stennis program, and the Federal University of Parana (UFPR).

References

Aji, A., Wang, F., Vo, H., Lee, H., Liu, Q., Zhang, X., Saltz, J., 2013. Hadoop gis: A high performance spatial data warehousing system over mapreduce. Proc. VLDB Endow. 6, 1009–1020. https://doi.org/10.14778/2536222.2536227

Alonzo, M., Bookhagen, B., Roberts, D.A., 2014. Urban tree species mapping using hyperspectral and lidar data fusion. Remote Sens. Environ. 148, 70–83. https://doi.org/10.1016/j.rse.2014.03.018

Alonzo, M., McFadden, J.P., Nowak, D.J., Roberts, D.A., 2016. Mapping urban forest structure and function using hyperspectral imagery and lidar data. Urban For. Urban Green. 17, 135–147. https://doi.org/10.1016/j.ufug.2016.04.003

Anderson, K., Gaston, K.J., 2013. Lightweight unmanned aerial vehicles will revolutionize spatial ecology. Front. Ecol. Environ. 11, 138–146. https://doi.org/10.1890/120150

Asner, G.P., Kellner, J.R., Kennedy-Bowdoin, T., Knapp, D.E., Anderson, C., Martin, R.E., 2013. Forest Canopy Gap Distributions in the Southern Peruvian Amazon. PLoS One 8. https://doi.org/10.1371/journal.pone.0060875

Campbell, M.J., Dennison, P.E., Hudak, A.T., Parham, L.M., Butler, B.W., 2018. Quantifying understory vegetation density using small-footprint airborne lidar. Remote Sens. Environ. 215, 330–342. https://doi.org/10.1016/j.rse.2018.06.023

Corona, P., Cartisano, R., Salvati, R., Chirici, G., Floris, A., di Martino, P., Marchetti, M., Scrinzi, G., Clementel, F., Travaglini, D., Torresan, C., 2012. Airborne laser scanning to support forest resource management under alpine, temperate and mediterranean environments in Italy. Eur. J. Remote Sens. 45, 27–37. https://doi.org/10.5721/EuJRS20124503

Cunha Neto, E.M. da, Nogueira Junior, M.R., Melo, M.R. da S., Rocha, J.E.C. da, 2019. Eucalyptus spp. volume determined through geospatial interpolation. Científica 47, 434–440. https://doi.org/10.15361/1984-5529.2019v47n4p434-440

Cunha Neto, E.M. da, Rocha, J.E.C. da, Bezerra, J.C.F., Melo, M.R. da S., Alves, G.A.R., 2020. Técnicas de interpolação geoespacial na estimativa do volume de Eucalyptus spp. na mesorregião sudeste paraense. Rev. Ibero-Americana Ciências Ambient. 11, 45–54. https://doi.org/10.6008/cbpc2179-6858.2020.005.0005

Donoghue, D.N.M., Watt, P.J., 2006. Using LiDAR to compare forest height estimates from IKONOS and Landsat ETM+ data in Sitka spruce plantation forests. Int. J. Remote Sens. 27, 2161–2175. https://doi.org/10.1080/01431160500396493

Feng, Q., Liu, J., Gong, J., 2015. UAV Remote sensing for urban vegetation mapping using random forest and texture analysis. Remote Sens. 7, 1074–1094. https://doi.org/10.3390/rs70101074

Guo, Q., Su, Y., Hu, T., Zhao, X., Wu, F., Liu, J., Chen, L., Xu, G., Lin, G., Zheng, Y., Lin, Y., Mi, X., Fei, L., Wang, X., 2017. An integrated UAV-borne lidar system for 3D habitat mapping in three forest ecosystems across China. Int. J. Remote Sens. 00, 1–19. https://doi.org/10.1080/01431161.2017.1285083

Haala, N., Brenner, C., 1999. Extraction of buildings and trees in urban environments. ISPRS J. Photogramm. Remote Sens. 54, 130–137. https://doi.org/10.1016/S0924-2716(99)00010-6

Hall, R.J., Skakun, R.S., Arsenault, E.J., Case, B.S., 2006. Modeling forest stand structure attributes using Landsat ETM+ data: Application to mapping of aboveground biomass and stand volume. For. Ecol. Manage. 225, 378–390. https://doi.org/10.1016/j.foreco.2006.01.014

Hamraz, H., Contreras, M.A., Zhang, J., 2017. Forest understory trees can be segmented accurately within sufficiently dense airborne laser scanning point clouds. Sci. Rep. 7, 1–9. https://doi.org/10.1038/s41598-017-07200-0

Holopainen, M., Kankare, V., Vastaranta, M., Liang, X., Lin, Y., Vaaja, M., Yu, X., Hyyppä, J., Hyyppä, H., Kaartinen, H., Kukko, A., Tanhuanpää, T., Alho, P., 2013. Tree mapping using airborne, terrestrial and mobile laser scanning - A case study in a heterogeneous urban forest. Urban For. Urban Green. 12, 546–553. https://doi.org/10.1016/j.ufug.2013.06.002

Hongchao, M., Wang, Z., 2011. Distributed data organization and parallel data retrieval methods for huge laser scanner point clouds. Comput. Geosci. 37, 193–201. https://doi.org/10.1016/j.cageo.2010.05.017

Jakubowski, M.K., Guo, Q., Kelly, M., 2013. Tradeoffs between lidar pulse density and forest measurement accuracy. Remote Sens. Environ. 130, 245–253. https://doi.org/10.1016/j.rse.2012.11.024

Jiang, B., Chang, C.Y., Sullivan, W.C., 2014. A dose of nature: Tree cover, stress reduction, and gender differences. Landsc. Urban Plan. 132, 26–36. https://doi.org/10.1016/j.landurbplan.2014.08.005

Jim, C.Y., 2004. Green-space preservation and allocation for sustainable greening of compact cities. Cities 21, 311–320. https://doi.org/10.1016/j.cities.2004.04.004

Kükenbrink, D., Schneider, F.D., Leiterer, R., Schaepman, M.E., Morsdorf, F., 2017. Quantification of hidden canopy volume of airborne laser scanning data using a voxel traversal algorithm. Remote Sens. Environ. 194, 424–436. https://doi.org/10.1016/j.rse.2016.10.023

La Rosa, D., Wiesmann, D., 2013. Land cover and impervious surface extraction using parametric and non-parametric algorithms from the open-source software R: An application to sustainable urban planning in Sicily. GIScience Remote Sens. 50, 231–250. https://doi.org/10.1080/15481603.2013.795307

Laurance, W.F., 2009. Conserving the hottest of the hotspots. Biol. Conserv. 142, 1137. https://doi.org/10.1016/j.biocon.2008.10.011

Li, J., Hu, B., Noland, T.L., 2013. Classification of tree species based on structural features derived from high density LiDAR data. Agric. For. Meteorol. 171–172, 104–114. https://doi.org/10.1016/j.agrformet.2012.11.012

Liu, C., Li, X., 2012. Carbon storage and sequestration by urban forests in Shenyang, China. Urban For. Urban Green. 11, 121–128. https://doi.org/10.1016/j.ufug.2011.03.002

Liu, J., Shen, J., Zhao, R., Xu, S., 2013. Extraction of individual tree crowns from airborne LiDAR data in human settlements. Math. Comput. Model. 58, 524–535. https://doi.org/10.1016/j.mcm.2011.10.071

Machado, S. do A., Santos, A.A.P. dos, Zamin, N.T., Nascimento, R.G.M., 2012. Spatial distribution of a Mixed Ombrophylus Forest fragment. Ciência Rural 42, 1013–1019. https://doi.org/10.1590/s0103-84782012005000029

McHale, M.R., Gregory McPherson, E., Burke, I.C., 2007. The potential of urban tree plantings to be cost effective in carbon credit markets. Urban For. Urban Green. 6, 49–60. https://doi.org/10.1016/j.ufug.2007.01.001

Means, J.E., Acker, S.A., Fltt, B.J., Renslow, M., Emerson, L., Hendrix, C.J., 2000. Predicting forest stand characteristics with Airborne Scanning Lidar. Photogramm. Eng. Remote Sens. 66, 1367–1371.

Myers, N., Mittermeier, R.A., Mittermeier, C.G., Fonseca, G.A.B. da, Kent, J., 2000. Biodiversity hotspots for conservation priorities. Nature 403, 853–858. https://doi.org/10.1038/35002501

Næsset, E., Økland, T., 2002. Estimating tree height and tree crown properties using airborne scanning laser in a boreal nature reserve. Remote Sens. Environ. 79, 105–115. https://doi.org/10.1016/S0034-4257(01)00243-7

Nowak, D.J., Crane, D.E., Stevens, J.C., Hoehn, R.E., Walton, J.T., Bond, J., 2008. A ground-based method of assessing urban forest structure and ecosystem services. Arboric. Urban For. 34, 347–358.

Peel, M.C., Finlayson, B.L., McMahon, T.A., 2007. Updated world map of the Köppen-Geiger climate classification. Hydrol. Earth Syst. Sci. 11, 1633–1644. https://doi.org/10.1002/ppp.421

Popescu, S.C., Wynne, R.H., 2004. Seeing the Trees in the Forest. Photogramm. Eng. Remote Sens. 70, 589–604. https://doi.org/10.14358/pers.70.5.589

R Core Team, 2019. R: A language and environment for statistical computing.

Rex, F.E., Corte, A.P.D., Machado, S. do A., Silva, C.A., Sanquetta, C.R., 2019. Estimating Above-Ground Biomass of Araucaria angustifolia (Bertol.) Kuntze Using LiDAR Data. Floresta e Ambient. 26. https://doi.org/10.1590/2179-8087.110717

Roussel, J.-R., Auty, D., 2019. lidR: Airborne LiDAR data manipulation and visualization for forestry applications.

Ruiz, L.A., Hermosilla, T., Mauro, F., Godino, M., 2014. Analysis of the influence of plot size and LiDAR density on forest structure attribute estimates. Forests 5, 936–951. https://doi.org/10.3390/f5050936

Saarinen, N., Vastaranta, M., Kankare, V., Tanhuanpää, T., Holopainen, M., Hyyppä, J., Hyyppä, H., 2014. Urban-tree-attribute update using multisource single-tree inventory.

Forests 5, 1032–1052. https://doi.org/10.3390/f5051032

Sankey, J.B., Ravi, S., Wallace, C.S.A., Webb, R.H., Huxman, T.E., 2012. Quantifying soil surface change in degraded drylands: Shrub encroachment and effects of fire and vegetation removal in a desert grassland. J. Geophys. Res. Biogeosciences 117, 1–11. https://doi.org/10.1029/2012JG002002

Sankey, T., Donager, J., Mcvay, J., Sankey, J.B., 2017. Remote Sensing of Environment UAV lidar and hyperspectral fusion for forest monitoring in the southwestern USA. Remote Sens. Environ. 195, 30–43. https://doi.org/10.1016/j.rse.2017.04.007

Sankey, T.T., Glenn, N., Ehinger, S., Boehm, A., Hardegree, S., 2010. Characterizing western juniper expansion via a fusion of Landsat 5 thematic mapper and lidar data. Rangel. Ecol. Manag. 63, 514–523. https://doi.org/10.2111/REM-D-09-00181.1

Sanquetta, C.R., Dalla Corte, A.P., Behling, A., De Oliveira Piva, L.R., Péllico Netto, S., Rodrigues, A.L., Sanquetta, M.N.I., 2018. Selection criteria for linear regression models to estimate individual tree biomasses in the Atlantic Rain Forest, Brazil 01 Mathematical Sciences 0104 Statistics. Carbon Balance Manag. 13. https://doi.org/10.1186/s13021-018-0112-6

Silva, C.A., Crookston, N.L., Hudak, A.T., Vierling, L.A., Klauberg, C., Cardil, A., 2017a. rLiDAR: LiDAR data processing and visualization.

Silva, C.A., Hudak, A.T., Vierling, L.A., Klauberg, C., Garcia, M., Ferraz, A., Keller, M., Eitel, J., Saatchi, S., 2017b. Impacts of airborne lidar pulse density on estimating biomass stocks and changes in a selectively logged tropical forest. Remote Sens. 9. https://doi.org/10.3390/rs9101068

Silva, C.A., Klauberg, C., Hudak, A.T., Vierling, L.A., Jaafar, W.S.W.M., Mohan, M., Garcia, M., Ferraz, A., Cardil, A., Saatchi, S., 2017c. Predicting stem total and assortment volumes in an industrial Pinus taeda L. forest plantation using airborne laser scanning data and random forest. Forests 8, 1–17. https://doi.org/10.3390/f8070254

Tigges, J., Lakes, T., Hostert, P., 2013. Urban vegetation classification: Benefits of multitemporal RapidEye satellite data. Remote Sens. Environ. 136, 66–75. https://doi.org/10.1016/j.rse.2013.05.001

Tooke, T.R., Coops, N.C., Goodwin, N.R., Voogt, J.A., 2009. Extracting urban vegetation characteristics using spectral mixture analysis and decision tree classifications. Remote Sens. Environ. 113, 398–407. https://doi.org/10.1016/j.rse.2008.10.005

Vivoni, E.R., Rango, A., Anderson, C.A., Pierini, N.A., Schreiner-Mcgraw, A.P., Saripalli, S., Laliberte, A.S., 2014. Ecohydrology with unmanned aerial vehicles. Ecosphere 5, 1–14. https://doi.org/10.1890/ES14-00217.1

Wallace, L., Lucieer, A., Watson, C., Turner, D., 2012. Development of a UAV-LiDAR system with application to forest inventory. Remote Sens. 4, 1519–1543. https://doi.org/10.3390/rs4061519

Wannasiri, W., Nagai, M., Honda, K., Santitamnont, P., Miphokasap, P., 2013. Extraction of mangrove biophysical parameters using airborne LiDAR. Remote Sens. 5, 1787–1808. https://doi.org/10.3390/rs5041787

Watt, M.S., Adams, T., Aracil, S.G., Marshall, H., Watt, P., 2013. The influence of LiDAR pulse density and plot size on the accuracy of New Zealand plantation stand volume equations. New Zeal. J. For. Sci. 43, 1–10. https://doi.org/10.1186/1179-5395-43-15

Watt, M.S., Meredith, A., Watt, P., Gunn, A., 2014. The influence of LiDAR pulse density on the precision of inventory metrics in young unthinned Douglas-fir stands during initial and subsequent LiDAR acquisitions. New Zeal. J. For. Sci. 44, 1–9. https://doi.org/10.1186/s40490-014-0018-3

Werder, S., Krüger, A., 2009. Parallelizing geospatial tasks in grid computing. GIS-Zeitschrift fur Geoinformatik 71–76.

Wilkinson, B., Lassiter, H.A., Abd-Elrahman, A., Carthy, R.R., Ifju, P., Broadbent, E., Grimes, N., 2019. Geometric targets for UAS lidar. Remote Sens. 11. https://doi.org/10.3390/rs11243019

Wu, B., Yu, B., Yue, W., Shu, S., Tan, W., Hu, C., Huang, Y., Wu, J., Liu, H., 2013. A voxel-based method for automated identification and morphological parameters estimation of individual street trees from mobile laser scanning data. Remote Sens. 5, 584–611. https://doi.org/10.3390/rs5020584

Yin, D., Wang, L., 2019. Individual mangrove tree measurement using UAV-based LiDAR data: Possibilities and challenges. Remote Sens. Environ. 223, 34–49. https://doi.org/10.1016/j.rse.2018.12.034

Zhang, C., Zhou, Y., Qiu, F., 2015. Individual tree segmentation from LiDAR point clouds for urban forest inventory. Remote Sens. 7, 7892–7913. https://doi.org/10.3390/rs70607892

Zhang, W., Qi, J., Wan, P., Wang, H., Xie, D., Wang, X., Yan, G., 2016. An easy-to-use airborne LiDAR data filtering method based on cloth simulation. Remote Sens. 8, 1–22. https://doi.org/10.3390/rs8060501

Zhang, X., Feng, X., Jiang, H., 2010. Object-oriented method for urban vegetation mapping using ikonos imagery. Int. J. Remote Sens. 31, 177–196. https://doi.org/10.1080/01431160902882603

Table 1. Descriptive statistics of the *A. angustifolia* UAV-Lidar derived tree height in an Urban Atlantic Forest

Scenarios		Statistic		
		Min	Mean	Max
Field-based		14.20	19.36 ± 1.63	24.00
Point cloud density (return.m^{-2})	2,500	16.23	20.5 5 ± 1.99	25.79
	1,000	16.25	20.51 ± 1.99	25.78
	500	16.17	20.46 ± 1.99	25.75
	250	16.19	20.39 ± 1.97	25.59
	100	15.90	20.27 ± 1.99	25.57
	50	16.02	20.15 ± 2.01	25.15
	25	15.75	19.93 ± 2.04	25.42
	10	14.61	19.8 5 ± 2.23	26.45
	5	11.86	19.25 ± 2.45	26.05

Table 2. Performance of different point densities when deriving *A. angustifolia* tree height in an Urban Atlantic Forest

Density	r	*RMSE* (m)	*rRMSE* (%)	Bias (m)	Bias (%)	χ^2	χ^2c
2,500	0.71	1.85	9.55%	-1.2	-6.18	30.23^{ns}	
1,000	0.71	1.82	9.42%	-1.15	-5.97	29.40^{ns}	
500	0.72	1.78	9.18%	-1.1	-5.68	27.88^{ns}	
250	0.72	1.72	8.9%	-1.03	-5.33	26.23^{ns}	
100	0.73	1.65	8.51%	-0.92	-4.74	23.89^{ns}	200.33
50	0.72	1.62	8.35%	-0.79	-4.09	22.90^{ns}	
25	0.67	1.63	8.43%	-0.57	-2.96	23.07^{ns}	
10	0.56	1.95	10.07%	-0.49	-2.53	32.67^{ns}	
5	0.44	2.27	11.71%	0.11	0.57	42.82^{ns}	

RMSE is root mean square error, r is Pearson correlation, χ^2 is calculated Chi-square test, χ^2c is critical Chi-square test, ns is not significant by the Chi-square test (95% probability).

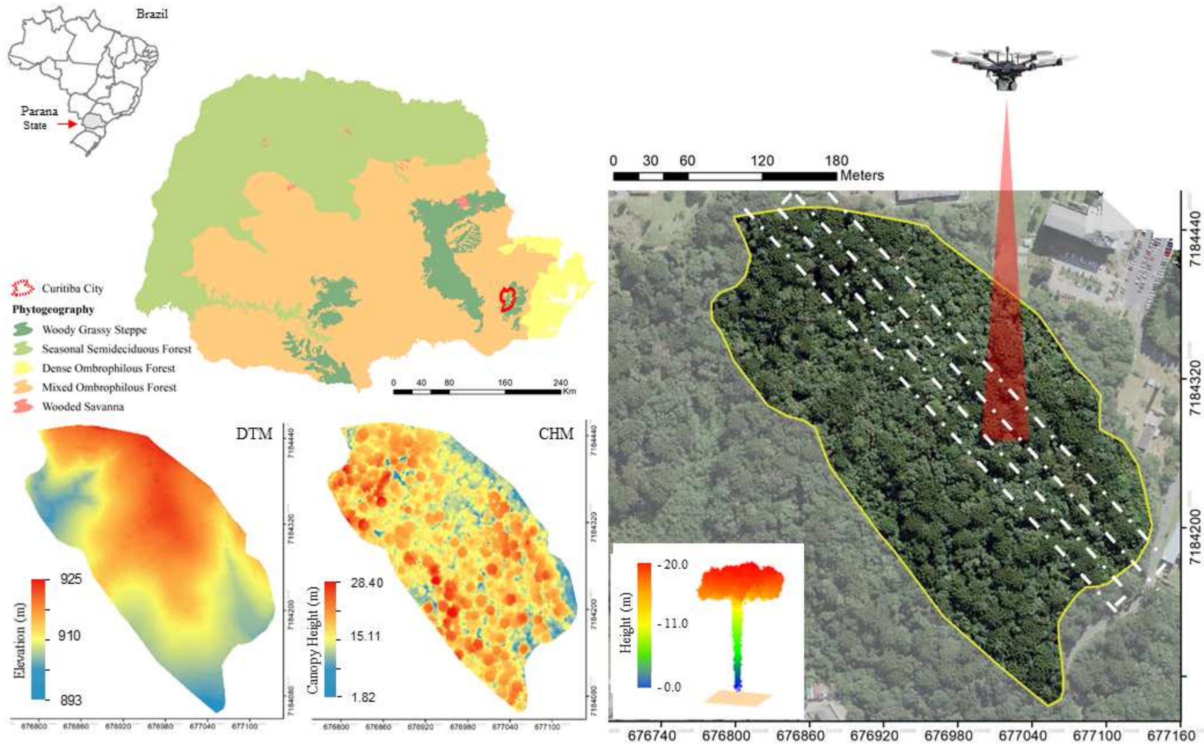

Fig. 1. Location of the study area in Curitiba, State of Paraná, southern Brazil

Note: DTM is the digital terrain model; CHM is the canopy height model.

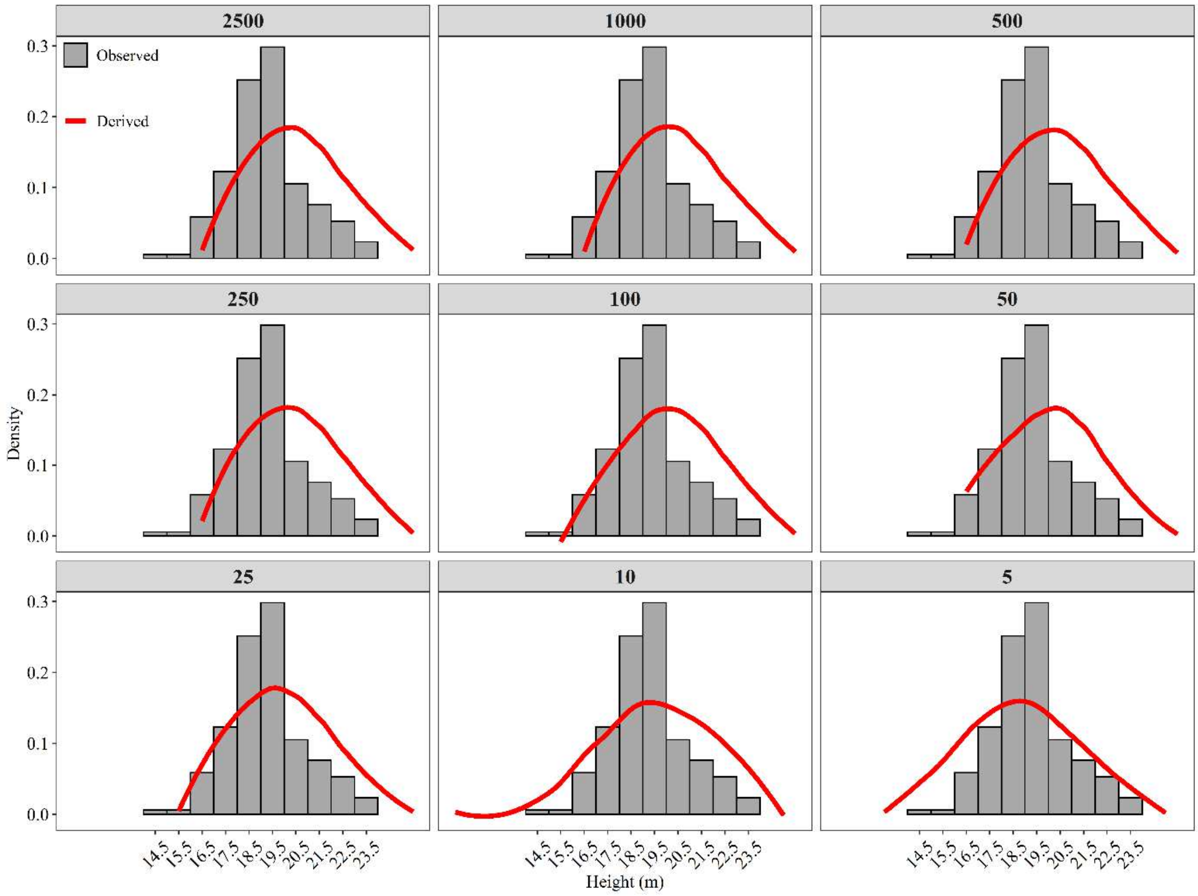

Fig. 2. Distribution of field-based and UAV-Lidar derived tree heights of *A. angustifolia* in an Urban Atlantic Forest

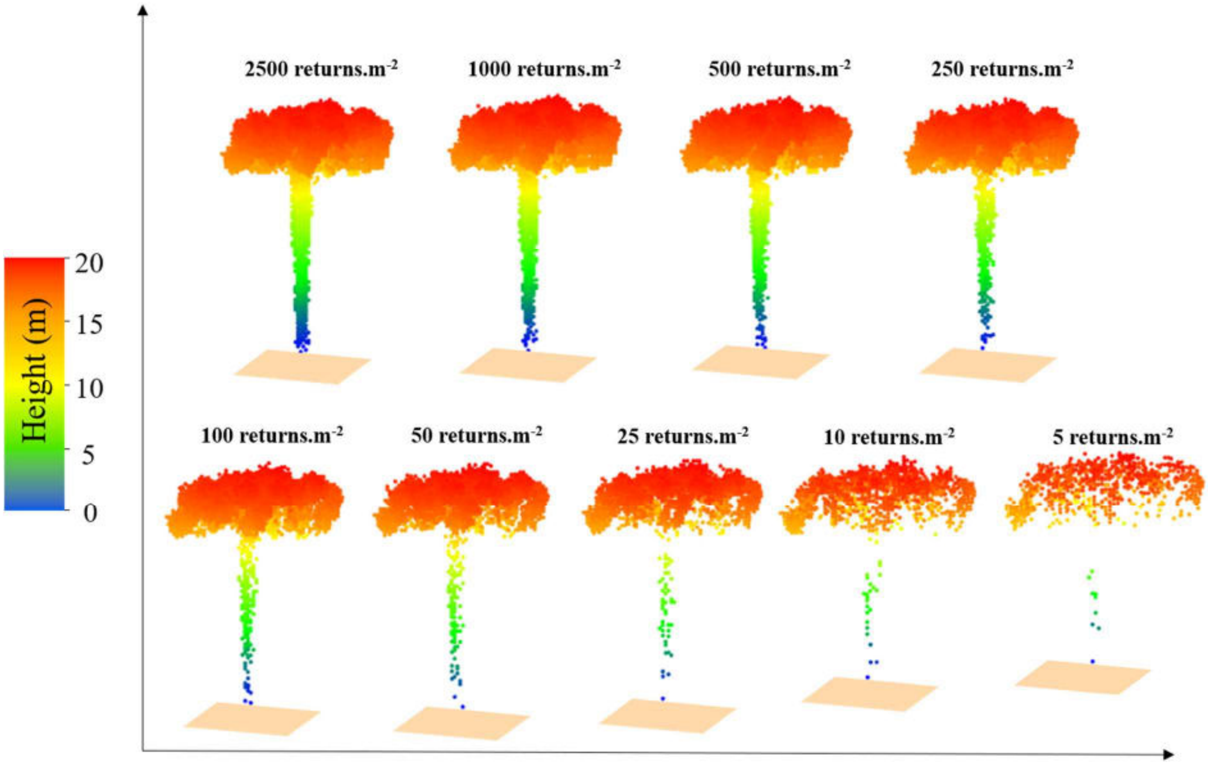

Fig. 3. *A. angustifolia* tree profile derived from UAV-Lidar point cloud in in an Urban Atlantic Forest

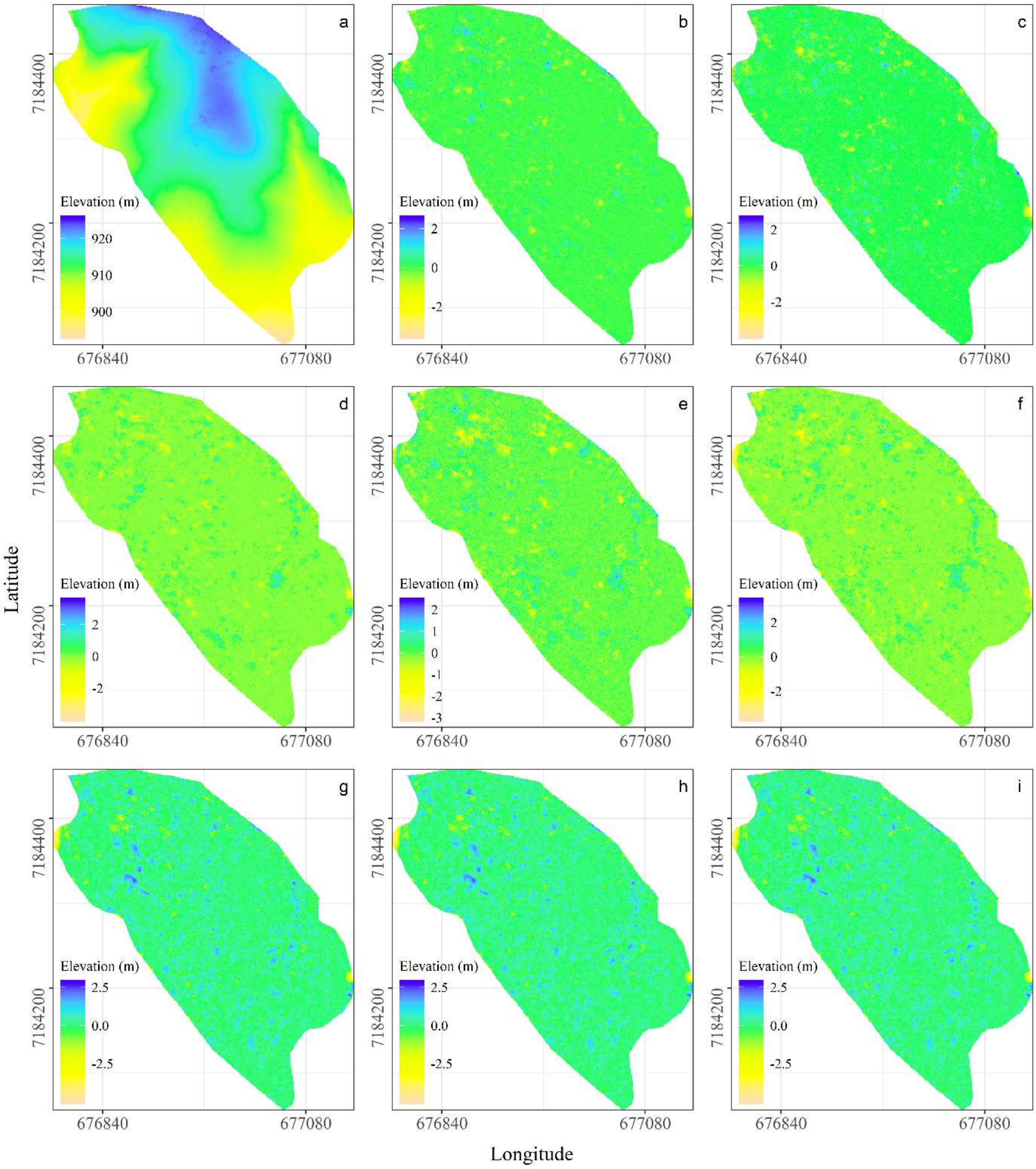

Fig. 4. Digital terrain model generated by the different point cloud density in the study area

Note: a) is a DTM with 2500 returns.m^{-2}; b) is the difference between the DTMs of 2,500 and 1,000 returns.m^{-2}; c is the difference between the DTMs of 2,500 and 500 returns.m^{-2}; d) is the difference between the DTMs of 2,500 and 250 returns.m^{-2}; e) is the difference between the DTMs of 2,500 and 100 returns.m^{-2}, f) is the difference between the DTMs of 2,500 and 50 returns.m^{-2}; g) is the difference between the DTMs of 2,500 and 25 returns.m^{-2}; h) is the difference between the DTMs of 2,500 and 10 returns.m^{-2}; and i) is the difference between the DTMs of 2,500 and 5 returns.m^{-2}.

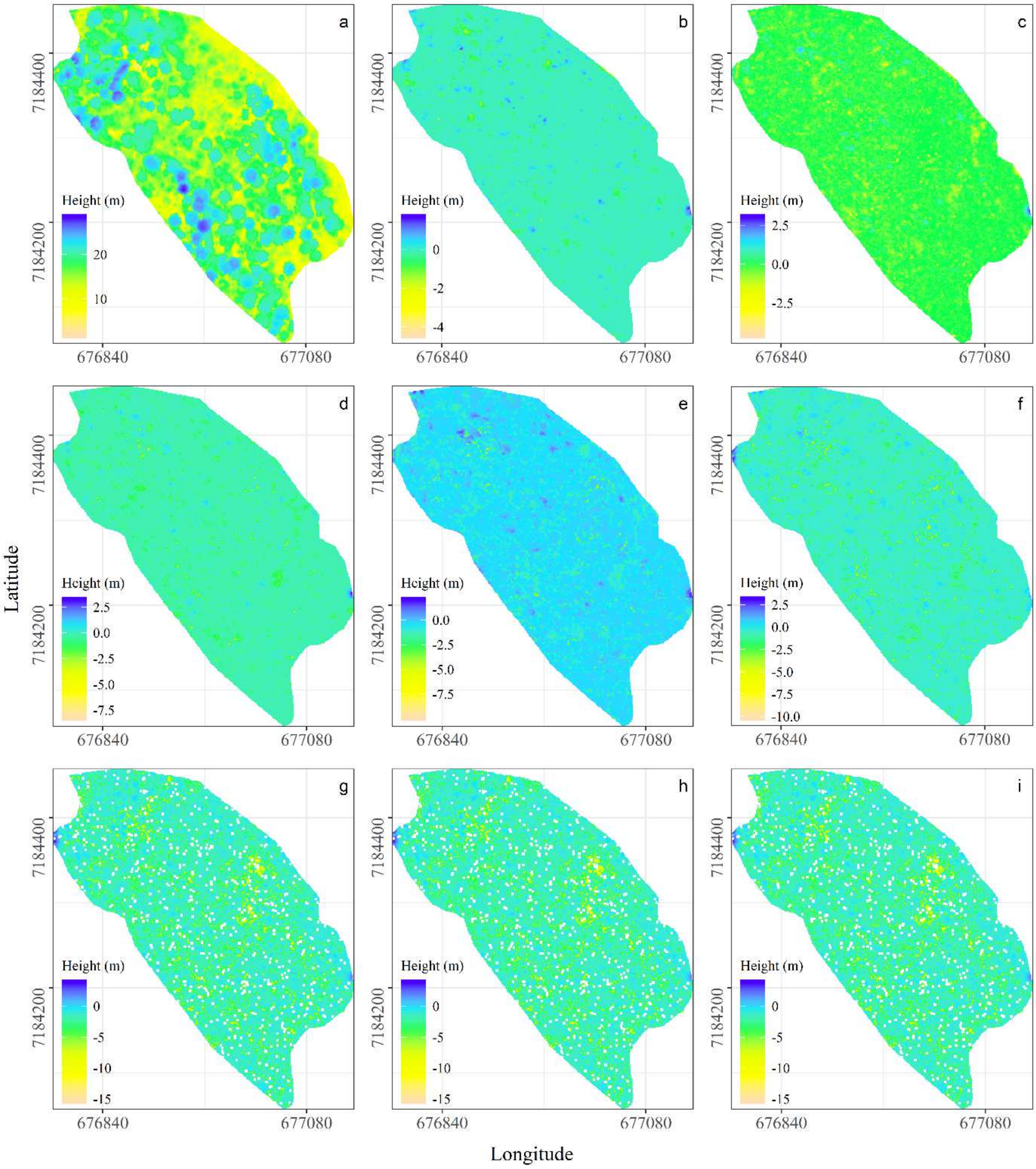

Fig. 5. Canopy height model generated by the different point cloud density in the study area

Note: a) is a CHM with 2,500 returns.m^{-2}; b) is the difference between the CHMs of 2,500 and 1,000 returns.m^{-2}; c) is the difference between the CHMs of 2,500 and 500 returns.m^{-2}; d) is the difference between the CHMs of 2,500 and 250 returns.m^{-2}; e) is the difference between the CHMs of 2,500 and 100 returns.m^{-2}; f) is the difference between the CHMs of 2,500 and 50 returns.m^{-2}; g) is the difference between the CHMs of 2,500 and 25 returns.m^{-2}; h) is the difference between the CHMs of 2,500 and 10 returns.m^{-2}; and i) is the difference between the CHMs of 2,500 and 5 returns.m^{-2}.

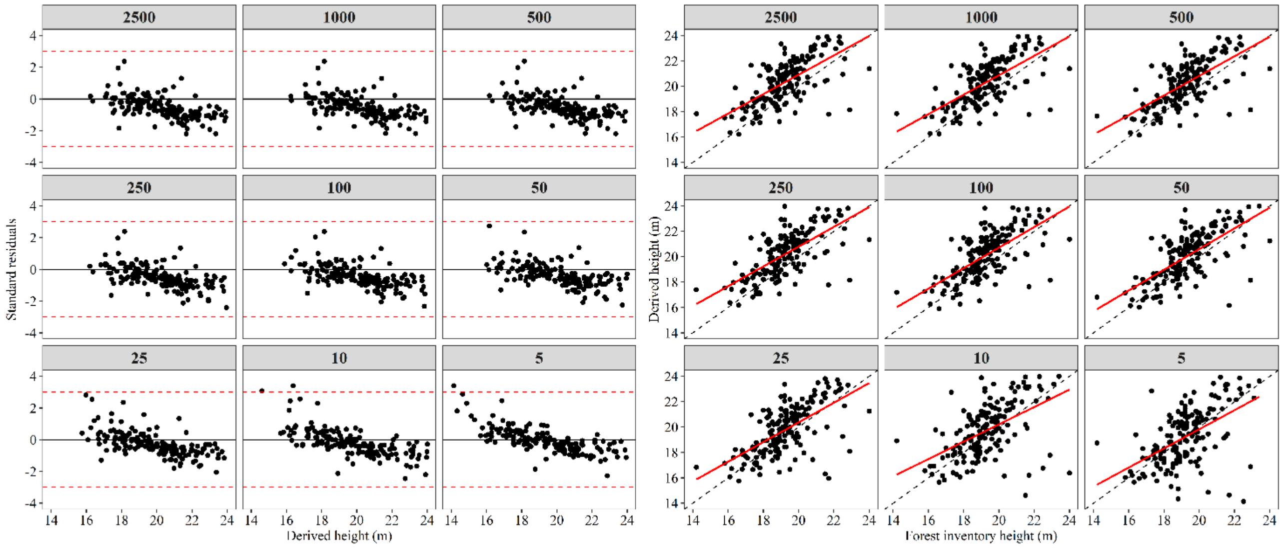

Fig. 6. Residuals and agreement between field-based and UAV-Lidar derived tree height of *A. angustifolia* in an Urban Atlantic Forest

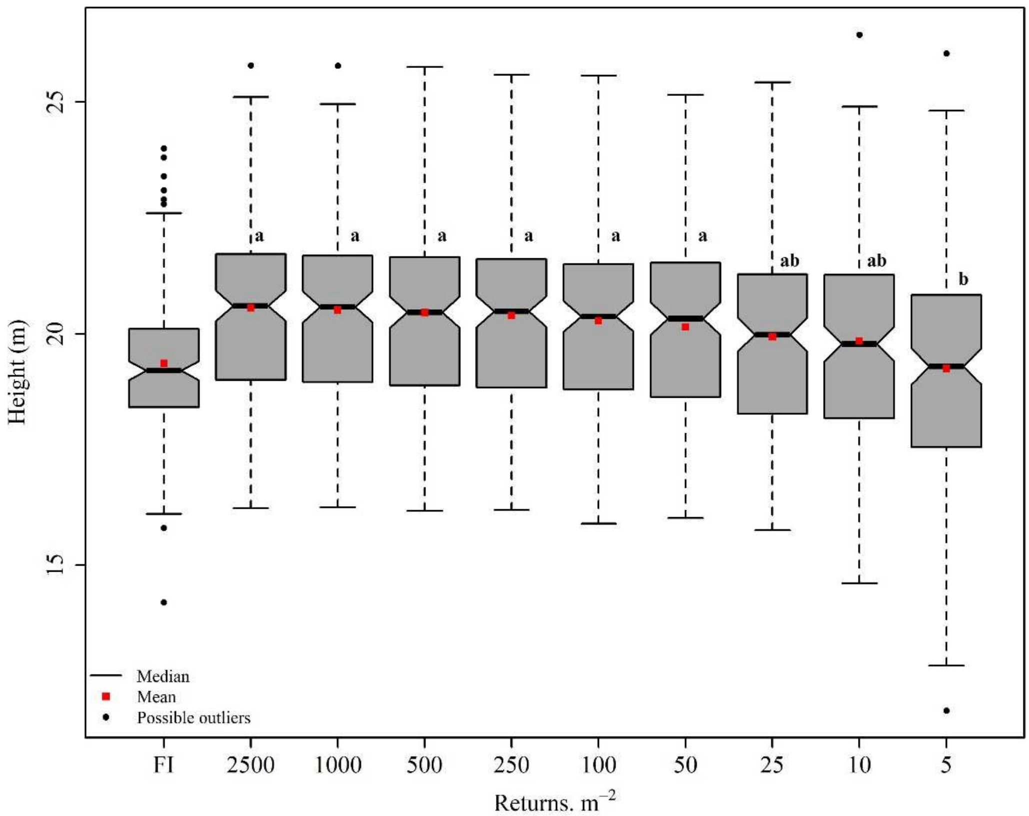

Fig. 7. Boxplot of UAV-Lidar derived tree heights of *A. angustifolia* using different point densities in an Urban Atlantic Forest

Note: Means followed by equal letters do not differ by Duncan test at 5% significance level.